

Electron paramagnetic resonance of a donor in aluminum nitride crystals

S. M. Evans, N. C. Giles, and L. E. Halliburton^{a)}

Department of Physics, West Virginia University, Morgantown, West Virginia 26506

G. A. Slack, S. B. Schujman, and L. J. Schowalter

Crystal IS, Incorporated, Green Island, New York 12183

(Received 6 November 2005; accepted 17 January 2006; published online 10 February 2006)

Electron paramagnetic resonance (EPR) and electron-nuclear double resonance (ENDOR) spectra are obtained from a donor in aluminum nitride (AlN) crystals. Although observed in as-grown crystals, exposure to x rays significantly increases the concentration of this center. ENDOR identifies a strong hyperfine interaction with one aluminum neighbor along the *c* axis and weaker equivalent hyperfine interactions with three additional aluminum neighbors in the basal plane. These aluminum interactions indicate that the responsible center is a deep donor at a nitrogen site. The observed paramagnetic defect is either a neutral oxygen substituting for nitrogen (O_N^0) or a neutral nitrogen vacancy (V_N^0). © 2006 American Institute of Physics. [DOI: 10.1063/1.2173237]

Single crystals of aluminum nitride (AlN) are excellent candidates for use as substrates in the epitaxial production of III-nitride electronic and optoelectronic devices.¹ Although significant progress has been made in the growth of bulk AlN crystals,^{2–6} the investigation of impurities and native defects in this material is still in a preliminary stage. It is widely acknowledged that oxygen is the primary unintentional impurity in AlN crystals^{7–11} and that native defects, such as nitrogen vacancies and aluminum vacancies, also exist.^{12–14} These oxygen impurities and native defects are present at significant concentrations in many AlN crystals, and can greatly influence the optical and electrical properties of the crystals. To maintain progress in the development of high-quality AlN substrates, it is important to use optical absorption, luminescence, and magnetic resonance to identify “characteristic” spectra for each of the major donors and acceptors. Results from these experiments will also complement the first-principles calculations that are being used to investigate the structure and energetics of point defects in the III-nitrides.¹⁵

Electron paramagnetic resonance (EPR), electron-nuclear double resonance (ENDOR), and optically detected magnetic resonance have proven to be effective techniques for identifying point defects in semiconductors. Only a few magnetic resonance studies, however, have been reported for AlN. Atobe *et al.*¹⁶ and Honda *et al.*¹⁷ attributed an EPR signal near $g=2.007$ in neutron-irradiated AlN ceramics to the nitrogen vacancy. In a separate investigation of AlN ceramics, Schweizer *et al.*¹⁸ suggested that an EPR signal near $g=2.004$ and its associated ENDOR was due to an oxygen on a nitrogen site with an adjacent aluminum vacancy and that a photoluminescence-EPR signal near $g=1.990$ was due to an isolated oxygen substituting for nitrogen. The ceramic nature of these samples^{16–18} did not allow the angular dependence of the spectra to be investigated. In contrast, Mason *et al.*¹⁹ used optically detected EPR to observe a series of $S=1$ and $S=1/2$ spectra in single crystals of AlN where angular dependence data were available. They suggested that one of their $S=1/2$ spectra (labeled D5, with $g_{\parallel}=2.001$ and

$g_{\perp}=2.007$) was associated with a displaced host aluminum atom.

In the present letter, we describe the results of an EPR and ENDOR study of single crystals of AlN. A broad EPR signal near $g=2.0$ is present in the as-grown crystals, and its intensity becomes much larger when a sample is irradiated at room temperature with x rays. Our ENDOR results show that this defect has a large hyperfine interaction with one ²⁷Al nucleus ($I=5/2$, 100% abundant) and weaker, but equivalent, hyperfine interactions with three other aluminum nuclei. The axial symmetry of this center and the hyperfine interactions with neighboring aluminums suggest that the responsible defect is an isolated donor on a nitrogen site, either a neutral oxygen substituting for nitrogen (O_N^0) or a neutral nitrogen vacancy (V_N^0). Our EPR spectrum appears to be the same as the D5 spectrum reported by Mason *et al.*,¹⁹ but we propose a different assignment. Mason *et al.*¹⁹ observed an increase in their D5 spectrum after irradiating with high-energy electrons, and suggested that an atomic displacement may have occurred. We see a similar increase in our signal during an irradiation with x rays, but consider only pre-existing defects as possible models for our center since the x rays are not expected to produce displacements in this material. We interpret our x-irradiation results as transient changes in charge states, lasting for hours or days at room temperature, that result from the capture of radiation-induced electrons and holes.

The bulk AlN crystals used in the present investigation were grown by a self-seeded sublimation-recondensation technique at Crystal IS (Green Island, NY). Small *c*-plate samples with typical dimensions of $5.0 \times 3.0 \times 1.3$ mm³ were cut from a larger boule. The EPR and ENDOR data were taken near 9.48 GHz using Bruker EMX and ELEXSYS spectrometers, respectively, while Oxford Instruments ESR-900 helium-gas-flow systems maintained the temperature of the samples at selected values in the 20 to 40 K range. Values of the static magnetic field were obtained with a proton gaussmeter. A small Cr-doped MgO crystal was used to correct for the difference in magnetic field between the sample and the probe tip of the gaussmeter (the isotropic g value for Cr³⁺ in MgO is 1.9800). The source of x rays was a Varian OEG-76H tube operating at 60 kV and 30 mA.

^{a)}Electronic mail: larry.halliburton@mail.wvu.edu

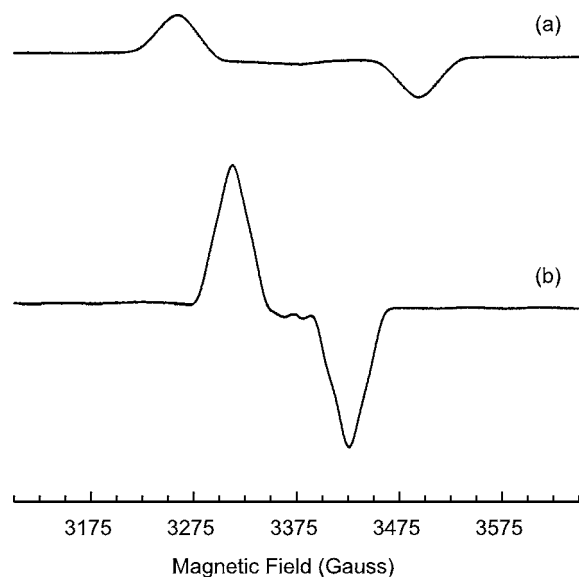


FIG. 1. EPR from a donor in a single crystal of AlN. This sample has been irradiated with x rays at room temperature to increase the intensity of the signal. These data were taken at 40 K with the magnetic field (a) parallel to the c axis and (b) perpendicular to the c axis. The microwave frequency was 9.480 GHz.

Our as-grown AlN crystals had a slight reddish color due to the presence of one or more weak defect-related optical absorption bands peaking in the 350 to 450 nm region. A small, but easily detected, EPR signal was also present in the as-grown crystals. Exposure to ionizing radiation (i.e., x rays) at room temperature for 30 min caused the EPR signal to increase by a factor between 5 and 10 (depending on the sample) and also caused the short-wavelength visible absorption to increase (making the sample appear more red to the eye). The EPR signal returned to its original intensity after several days if the sample was kept in the dark at room temperature. This restoration occurred in hours at room temperature if the sample was held in room light. Figure 1 shows the EPR spectra taken at 40 K with the magnetic field parallel and perpendicular to the crystal's c axis. The absorption curve represented by the EPR signal has a "top hat" shape which makes the first derivative shown in Fig. 1 extend up at lower field, stay near zero for a center field region, and extend down at higher field. These signals in Fig. 1 correspond to a concentration of spins of approximately $7 \times 10^{18} \text{ cm}^{-3}$. There is a slight shift of the center of our EPR spectrum when the magnetic field is rotated from the c axis to the basal plane, and no shift when the magnetic field is rotated within the basal plane. This indicates an axial g matrix. By choosing the centers of the two spectra in Fig. 1 to be midway between the upper and lower peaks on each side, we found that $g_{\parallel} = 2.002$ and $g_{\perp} = 2.006$.

The width of the spectrum in Fig. 1 changes significantly as the magnetic field is rotated from the c axis to the basal plane (approximately 238 G when the field is parallel to the c axis and 116 G when the field is perpendicular to the c axis). The ENDOR spectrum shown in Fig. 2 (taken with the magnetic field perpendicular to the c axis) and its angular dependence shown in Fig. 3 explain this variation in width. There is a large hyperfine interaction with one aluminum nucleus, as illustrated by the two sets of five lines centered at 23.31 and 31.05 MHz in Fig. 2. The 7.74 MHz separation of these two sets (located at $A/2 \pm \nu_N$) agrees with the predic-

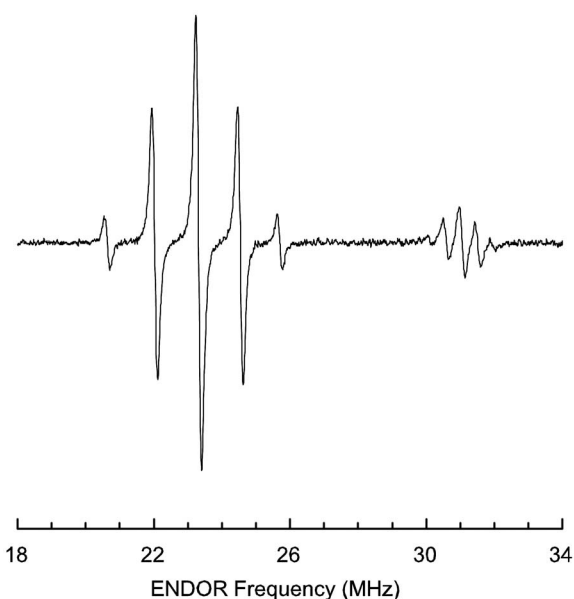


FIG. 2. ENDOR spectrum showing the primary aluminum interaction. These data were taken at 22 K with the magnetic field (3382 G) perpendicular to the c axis. The five lines in each set result from the nuclear electric quadrupole interaction for an $I=5/2$ nucleus.

tion of 7.51 MHz for $2\nu_N$ for the "free" ^{27}Al nucleus at 3382 G. Additional evidence that the ^{27}Al nucleus is responsible for the ENDOR spectrum in Fig. 2 comes from the five lines in each set. These lines arise from a nuclear electric quadrupole interaction and require an $I=5/2$ nucleus. The ENDOR spectrum in Fig. 2 does not change when the magnetic field is rotated in the basal plane, thus indicating axial hyperfine and nuclear electric quadrupole matrices with the unique axis oriented parallel to the c axis.

The following spin Hamiltonian (with $S=1/2, I=5/2$) describes the observed EPR and ENDOR spectra (Figs. 1 and 2), and is used to analyze the angular dependence shown in Fig. 3.

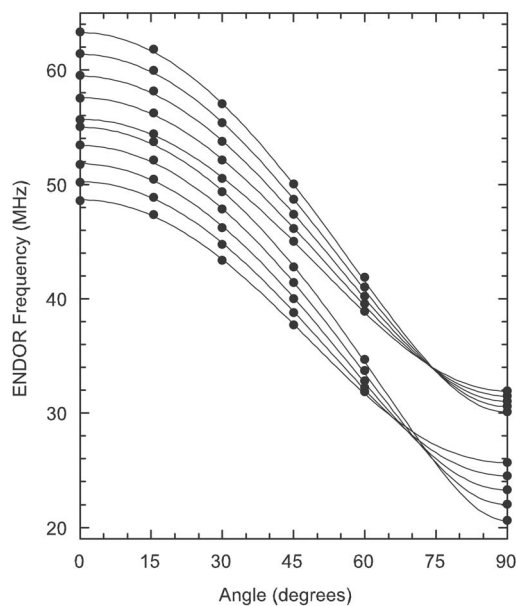


FIG. 3. Angular dependence of the primary aluminum ENDOR spectrum. The magnetic field was rotated from the c axis (0°) to the basal plane (90°). The solid lines are calculated using the best fit parameters and the discrete points represent experimental data.

$$H = \beta \mathbf{S} \cdot \mathbf{g} \cdot \mathbf{H} + \mathbf{I} \cdot \mathbf{A} \cdot \mathbf{S} + \mathbf{I} \cdot \mathbf{Q} \cdot \mathbf{I} - g_N \beta_N \mathbf{I} \cdot \mathbf{H}.$$

Only three parameters (A_{\parallel} , A_{\perp} , and P) are needed for this axial system. The Q matrix is traceless with $Q_{xx} = -P$, $Q_{yy} = -P$, and $Q_{zz} = 2P$. The parameter P is defined as $e^2 q Q / [4I(2I-1)]$, where eq is the electric field gradient and Q is the nuclear quadrupole moment. Fitting to the data points in Fig. 3 gave $A_{\parallel} = 111.30$ MHz, $A_{\perp} = 54.19$ MHz, and $P = 0.289$ MHz. The solid curves in Fig. 3 were then generated using these “best fit” values of the parameters. We could only determine the relative signs of the hyperfine and nuclear quadrupole parameters, and have assigned a positive sign to A_{\parallel} because the nuclear g factor for ^{27}Al is positive. The most striking feature of this large aluminium hyperfine interaction is its significant anisotropy.

In addition to the large hyperfine interaction with the one aluminum neighbor along the c axis, this center has weaker equivalent hyperfine interactions with the three aluminum neighbors in the basal plane. Details of these interactions will be presented in a later paper. With the magnetic field parallel to the c axis, the three aluminum nuclei in the basal plane have equivalent interactions, as verified by our observation of two sets of ENDOR lines located at $A/2 \pm \nu_N$ (each set contains five nuclear-quadrupole-split lines). The centers of the two sets were at 6.19 and 12.85 MHz for a magnetic field of 3381 G. Their separation of 6.66 MHz is in reasonable agreement with the expected ^{27}Al value of 7.51 MHz for $2\nu_N$ at this field. We used ENDOR-induced EPR (EI-EPR) to verify that all ten components within these two sets of lines were associated with the EPR spectrum shown in Fig. 1(a). The EI-EPR experiments also showed that other weak c -axis ENDOR lines appearing in the 7.4 to 15 MHz region were due to one or more separate broad EPR signals underlying our primary EPR signal. With the magnetic field parallel to an a axis, only two of the three hyperfine interactions with the aluminum neighbors in the basal plane are equivalent. For an arbitrary direction of field in the basal plane, all three aluminum interactions are inequivalent. When the magnetic field was rotated in the basal plane, ENDOR lines from all three basal-plane aluminums were observed and the centers of the high-frequency groups (i.e., those that correspond to $A/2 + \nu_N$) stayed between 8 and 13 MHz. The observed spectra repeated every 60° for rotation in this plane. We also found that the high-frequency groups stayed below 13 MHz when we rotated from the c axis to the basal plane. These results from the two planes suggest that the principal values of the hyperfine matrices describing the interactions with the basal-plane aluminums are in the 8 to 20 MHz range.

Our ENDOR results have demonstrated that the defect associated with the EPR signal in Fig. 1 interacts strongly with aluminum nuclei. This suggests that the responsible defect is located at a nitrogen site and thus is a donor, with substitutional oxygen impurities or nitrogen vacancies as the most likely candidates. The neutral charge state of the substitutional oxygen donor (O_N^0) and the neutral charge state of the nitrogen vacancy donor (V_N^0) are both expected to be paramagnetic with $S = 1/2$. Before irradiation with x rays, the majority of these donors in our crystals were in the nonparamagnetic singly ionized charge state (either O_N^+ or V_N^+). Only

a relatively small portion were in the neutral charge state, thus accounting for the weak EPR signal seen in the as-grown crystals. Since a crystal must always be electrically neutral, these singly ionized donors in the as-grown crystals are most likely compensated for by singly ionized or doubly ionized aluminum vacancies (V_{Al}^- and/or $\text{V}_{\text{Al}}^{2-}$). Exposure to x rays (ionizing radiation) at room temperature then converts the singly ionized donors to the paramagnetic neutral state by trapping a radiation-induced electron, while the corresponding radiation-induced hole is trapped elsewhere in the crystal. The identity of this trapping site for the holes is unknown, although the most likely possibilities are the singly and doubly ionized aluminum vacancies, which would convert to the V_{Al}^0 and V_{Al}^- charge states upon capturing a hole.

In summary, we have observed a broad EPR signal in as-grown single crystals of AlN. Ionizing radiation at room temperature significantly increases the concentration of the defect and causes the crystal to have a deeper reddish color. The paramagnetic center has the axial symmetry of the lattice, and ENDOR reveals a large hyperfine interaction with its axial aluminum neighbor and weaker equivalent hyperfine interactions with its three basal plane aluminum neighbors. We suggest that the defect responsible for the observed EPR and ENDOR spectra is a neutral donor, either an isolated substitutional oxygen O_N^0 or an isolated nitrogen vacancy V_N^0 .

This work was supported at West Virginia University by the National Science Foundation (Grant No. DMR-0508140). One of the authors (S.M.E.) received support from the WV EPSCoR STEM fellowship program.

- ¹M. Asif Khan, M. Shatalov, H. P. Maruska, H. M. Wang, and E. Kuokstis, *Jpn. J. Appl. Phys., Part 1* **44**, 7191 (2005).
- ²G. A. Slack and T. F. McNelly, *J. Cryst. Growth* **34**, 263 (1976); **42**, 560 (1977).
- ³J. C. Rojo, G. A. Slack, K. Morgan, B. Raghobhamachar, M. Dudley, and L. J. Schowalter, *J. Cryst. Growth* **231**, 317 (2001).
- ⁴R. Schlessler and Z. Sitar, *J. Cryst. Growth* **234**, 349 (2002).
- ⁵J. C. Rojo, L. J. Schowalter, R. Gaska, M. Shur, M. A. Khan, J. Yang, and D. D. Koleske, *J. Cryst. Growth* **240**, 508 (2002).
- ⁶M. Strassburg, J. Senawiratne, N. Dietz, U. Haboek, A. Hoffmann, V. Noveski, R. Dalmau, R. Schlessler, and Z. Sitar, *J. Appl. Phys.* **96**, 5870 (2004).
- ⁷T. Mattila and R. M. Nieminen, *Phys. Rev. B* **54**, 16676 (1996).
- ⁸C. G. Van de Walle, *Phys. Rev. B* **57**, R2033 (1998).
- ⁹G. A. Slack, L. J. Schowalter, D. Morelli, and J. A. Freitas, Jr., *J. Cryst. Growth* **246**, 287 (2002).
- ¹⁰J. A. Freitas, Jr., G. C. B. Braga, E. Silveira, J. G. Tischler, and M. Fatemi, *Appl. Phys. Lett.* **83**, 2584 (2003).
- ¹¹M. Bickermann, B. M. Epelbaum, and A. Winnacker, *Phys. Status Solidi C* **0**, 1993 (2003).
- ¹²Q. Zhou, M. O. Manasreh, M. Pophristic, S. Guo, and I. T. Ferguson, *Appl. Phys. Lett.* **79**, 2901 (2001).
- ¹³Q. Zhou and M. O. Manasreh, *Appl. Phys. Lett.* **80**, 2072 (2002).
- ¹⁴C. Stampfl and C. G. Van de Walle, *Phys. Rev. B* **65**, 155212 (2002).
- ¹⁵C. G. Van de Walle and J. Neugebauer, *J. Appl. Phys.* **95**, 3851 (2004).
- ¹⁶K. Atobe, M. Honda, N. Fukuoka, M. Okada, and M. Nakagawa, *Jpn. J. Appl. Phys., Part 1* **29**, 150 (1990).
- ¹⁷M. Honda, K. Atobe, N. Fukuoka, M. Okada, and M. Nakagawa, *Jpn. J. Appl. Phys., Part 2* **29**, L652 (1990).
- ¹⁸S. Schweizer, U. Rogulis, J.-M. Spaeth, L. Trinkler, and B. Berzina, *Phys. Status Solidi B* **219**, 171 (2000).
- ¹⁹P. M. Mason, H. Przybylinska, G. D. Watkins, W. J. Choyke, and G. A. Slack, *Phys. Rev. B* **59**, 1937 (1999).